Improved Source/Absorber Preparation for Radionuclide Spectrometry Based on Low-Temperature Calorimetric Detectors

L. Bockhorn[1,2] · M. Paulsen[3,4] · J. Beyer[3] · K. Kossert[1] · M. Loidl[5] ·
O. J. Nähle[1] · P. C.-O. Ranitzsch[1] · M. Rodrigues[5]

Abstract

High-resolution beta spectrometry based on low-temperature calorimetric detectors requires high-quality source/absorber combinations in order to avoid spectrum artifacts and to achieve optimal detection efficiency. In this work, preparation techniques and quality control methods to fabricate reliable source/absorber assemblies with the radionuclide under investigation embedded into them are discussed.

Keywords Beta spectrometry · Preparation techniques · Low-temperature detectors

1 Introduction

Energy-dispersive low-temperature detectors (LTDs) enable radionuclide spectrometry with energy resolutions and thresholds far exceeding those of conventional detectors such as lithium-drifted silicon detectors. Metallic magnetic calorimeters (MMCs) [1–3] are LTDs which have proven to be among the best detectors for beta spectrometry, especially at low energies [4,5]. For MMC-based beta spectra measurements, high-quality sources are needed to avoid spectrum artifacts and to achieve optimal detection efficiency.

✉ L. Bockhorn
  bockhorn@nano.uni-hannover.de

1   Physikalisch-Technische Bundesanstalt Braunschweig, Bundesallee 100, 38116 Braunschweig, Germany

2   Institut für Festkörperphysik - Abteilung Nanostrukturen, Gottfried Wilhelm Leibniz Universität Hannover, 30167 Hannover, Germany

3   Physikalisch-Technische Bundesanstalt Berlin, Abbestraße 2-12, 10587 Berlin, Germany

4   Kirchhoff-Institute for Physics, Im Neuenheimer Feld 227, 69120 Heidelberg, Germany

5   CEA, LIST, Laboratoire National Henri Becquerel, CEA Saclay, 91191 Gif-sur-Yvette Cedex, France
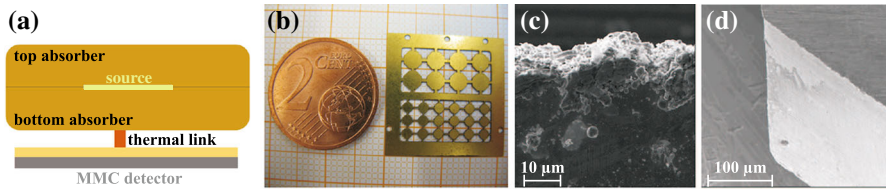
Fig. 1 (Color figure online) **a** Schematic cross section of a 4π absorber with embedded radionuclide source mounted on a MMC detector. **b** An absorber array (21 mm×21 mm) for the two largest absorber types. SEM images of absorber elements defined by laser cutting which may result in the formation of gold bulges (**c**) and milling **d** which produces well-defined edges

Ideally, the radionuclide under investigation is completely embedded into an absorber material—typically a noble metal—to ensure that every decay as well as the total decay energy is detected [6,7]. Such a source/absorber element, which fulfills a 4π geometry, is glued with Stycast 1266 onto thermal Au posts of the MMC detector, see, e.g., Paulsen et al. [7]. While the two-component adhesive dries at room temperature, a force of approximately 10 N is applied to ensure a tight thermal connection. Typically, these detectors have a 10/90 rise time of $\sim 50\,\mu s$ and a 90/10 fall time of $\sim 10\,ms$. The deposited activity is thus set to 2–5 Bq such that a reasonable number of decays can be detected while the number of expected pileup events is kept small $\sim 4\%$. For high-energy beta spectra ($E_{max} \geq 300\,keV$), it is advantageous to use layers of different materials as absorbers, so-called bilayers, in order to reduce the effect of bremsstrahlung escape. Conceptually, bilayer absorbers were mentioned in Paulsen et al. [7]. However, in this work we present a newly developed multi-step process for successfully fabricating them. Furthermore, we describe novel aspects of radionuclide-specific source preparation and applications of control methods that are needed for quality checks.

The paper is organized as follows. In Sect. 2, we present the source and absorber preparation for low- and high-energy beta spectra including single and bilayer absorbers. Section 3 concerns the source control and quality checks using radiographic imaging and activity measurements. A conclusion is provided in Sect. 4.

2 Source and Absorber Preparation

The source and absorber preparation is divided into three parts: (i) choosing, designing and fabricating the absorber material in Sects. 2.1 and 2.2 , (ii) depositing the radionuclide under investigation onto the absorber material and checking its quality in Sect. 2.3 and (iii) ensuring a 4π detection geometry as shown in Fig. 1a, and two absorbers are diffusion welded in Sect. 2.4.

2.1 Absorber Design and Fabrication

Fabricating an array of source/absorber elements increases the preparation efficiency while simplifying the handling during the preparation steps. Following the fabrication, individual source/absorbers can be selected, separated and mounted onto MMC

sensors. The structuring of the absorber array requires materials which are easy to machine, available in a highly pure form and chemically stable. Noble metals such as gold or silver meet these requirements. Furthermore, they exhibit a high stopping power for emitted particles and radiation and allow a fast thermalization of the decay energy. A structured absorber array is shown in Fig. 1b. Structuring the absorber arrays by laser cutting is suitable for thin gold foils (thickness $d < 90\,\mu\text{m}$). However, residues of evaporated gold may form bulges on the edges, see Fig. 1c. The formation of gold bulges may become critical as these can damage the MMC chip when the source/absorber elements are mounted. Milling of Au foils is suitable for thicker gold foils ($d \geq 90\,\mu\text{m}$) and provides well-defined edges as depicted in Fig. 1d. Milling of thinner gold foils was found to be unreliable due to possible mechanical damage. We have to weigh the advantages and disadvantages of both processes to achieve high-quality sources. Thus, for thin foils ($d < 30\,\mu\text{m}$) we used laser cutting and for thicker gold foils ($d \geq 90\,\mu\text{m}$) milling.

2.2 Absorber Design and Fabrication for Higher Energies ($E_{\text{max}} \geq 300$ keV)

Beta spectra with high endpoint energies ($E_{\text{max}} \geq 300\,\text{keV}$) measured with MMCs may be distorted by energy escape processes. Even if a high initial energy beta electron itself is stopped within a given absorber, bremsstrahlung photons may escape. This effect may cause decay events with high energies to be detected as lower energy decays. The probability of bremsstrahlung production increases with the electron energy and the atomic mass of the material in which the electron decelerates. Hence, a low atomic mass absorber material can reduce the number of generated bremsstrahlung photons. However, this has two disadvantages: (i) a larger absorber with higher heat capacity is then required, degrading the energy resolution and heightening the energy threshold of the detector, (ii) the photon absorption probability of a low atomic mass absorber material is lower, partially counteracting the advantage of the reduced bremsstrahlung production. A better result is achieved with a bilayer absorber [8]. Here, an inner low atomic mass layer reduces bremsstrahlung production where the electrons still have high energies and a high atomic mass outer layer reduces the total absorber thickness required for stopping the electrons while enhancing the photon absorption probability.

2.2.1 Simulations of Bilayer Absorbers

Using the Monte Carlo software EGSnrc [9], several simulations were carried out to compare the energy escape reduction capacity of different absorber configurations. The simulated tracks of 10^3 electrons with initial energy 800 keV started from an isotropic point-like source at the center of the absorber. The promising configurations are shown in Fig. 2: a Au-absorber, $d = d_{\text{Au}} = 300\,\mu\text{m}$; b Au–Cu-absorber, $d_{\text{Au}} = 200\,\mu\text{m}$ and $d_{\text{Cu}} = 150\,\mu\text{m}$; c Au–Cu–Au-absorber, $d_{\text{Au}} = 200\,\mu\text{m}$, $d_{\text{Cu}} = 150\,\mu\text{m}$ and $d_{\text{Au}} = 50\,\text{nm}$. The third configuration was simulated to obtain an upper bound for the effect of adding the thin layer of AuPd. Qualitatively, the Au-absorber has better stopping power for the electrons but more photons escape. The opposite is the case for the Au–Cu- and Au–Cu–Au-absorber. These features become more obvious when performing
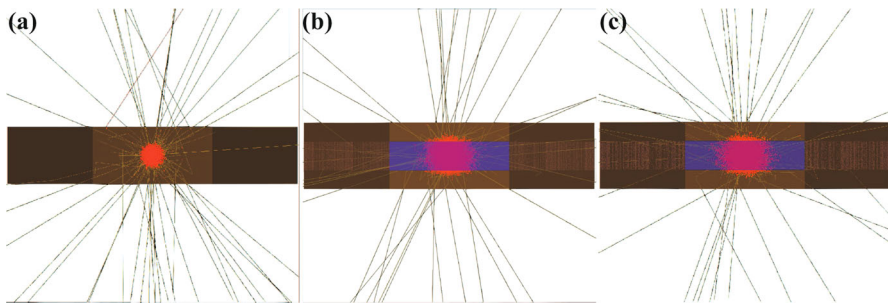
Fig. 2 (Color figure online) Plots of 10^3 simulated tracks for electrons (red) having initial energies 800 keV, showing the cross sections for three absorber configurations: **a** Au-absorber, **b** Au–Cu-absorber and **c** Au–Cu–Au-absorber. The photon tracks are also depicted

a quantitative simulation to record the photon escape, which indicates that a bilayer absorber reduces the energy escape by approximately 57% for 800 keV electrons.

2.2.2 Bilayer Absorber Fabrication

Preparation of Au–Cu bilayers is possible by means of diffusion welding. Since Cu tends to oxidize at elevated temperatures, it is advisable to carry out this process in a nearly oxygen-free atmosphere. Therefore, the welding oven needs to be evacuated and/or purged with inert gas before and during the bilayer fabrication. Gold and copper form continuous solid alloys over a large temperature range. The minimum melting temperature of these solutions is 910 °C. Nevertheless, even at lower temperatures diffusion of atoms at an interface can form a solid connection between the layers. Native surface oxide layers from the Cu foil must be removed directly prior to the diffusion welding using a combination of mechanical polishing and 15 min of wet etching in weak acids. An assembly of two aluminum halves with four clamping screws is needed to apply a defined pressure onto Cu–Au bilayer during the diffusion welding process. Suitable process parameters for a 24 mm × 24 mm Au–Cu bilayer foil are atmosphere: argon, torque per screw: 6.2 Nm, oven temperature: 500 °C, process time: 1 h to reach 500 °C + 1 h at 500 °C. Since exposing the foils to ambient atmosphere after the Au–Cu bilayer preparation is practically unavoidable, native Cu surface oxide will reform which must be removed again. To avoid this problem during source deposition, a comparably thin, e.g., 50 nm, non-oxidizing capping layer can be deposited onto the Cu surface. Gold or gold alloys, e.g., AuPd, are suitable capping layer materials. For practicality, the preparation of the Cu–Au bilayer foils should occur before formatting the absorber array.

2.3 Drop Deposition by Automated Microdispensing System and Source Quality Check

There are several methods to deposit a radionuclide into an absorber material such as ion implantation [10] and electrodeposition [6]. The simplest way to produce radionuclide sources is by drop deposition via manual pipetting. Limited control with regard to
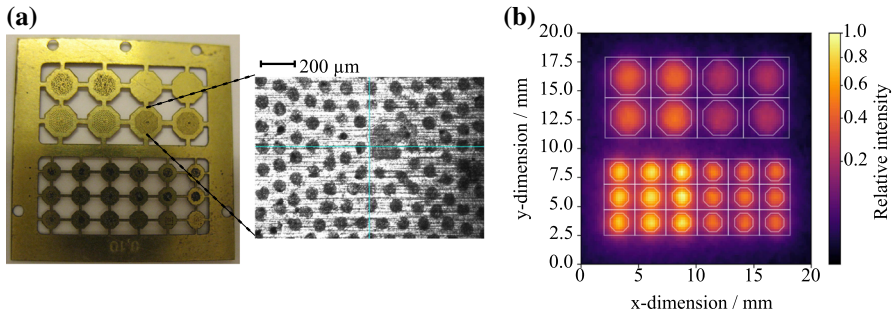
Fig. 3 (Color figure online) **a** Drop disposition done by a microdispensing system, a total volume of 0.5 μl was dispensed in a typical drop pattern. **b** After dispensing, the unsealed source is controlled by autoradiography. Two different activities (left half: 5 Bq, right half: 2.5 Bq) are seen

volume (~ 0.1 ml), activity and placement (~ 0.5 mm) may lead to source/absorbers of poor quality when using manual drop depositions. To avoid these problems, we utilize an automated microfluidic dispensing system [7] which can deposit radionuclide containing solutions with a placement accuracy of 20 μm and drop volumes of around 200 pl. Microfluidic dispensing systems easily enable drop pattern dispensing, see Fig. 3a which may be helpful to limit crystal growth caused by the salt load of the radionuclide carrier solution [6]. The drop-to-drop distance should be large enough to avoid overlaps. Also, the deposited drop needs to have dried before a new drop can be deposited at the same location. Typically, a drop with a volume of 200 pl dries within a few seconds. One problem when fabricating source/absorber assemblies is that the deposited activity may not be known until the final spectrometer measurement. Therefore, after a dispensing cycle, the deposited activity of the sources should be controlled. This can be done by autoradiography, a technique using x-ray film to visualize decay emissions from radioactive materials [11]. Autoradiographic images allow to estimate the position and activity of the radionuclide material deposited onto the individual absorber array elements as shown in Fig. 3b.

2.4 Diffusion Welding

The deposited radionuclide is embedded into the absorber material by diffusion welding a second absorber array onto the first one. A press consisting of two halves made of aluminum, four screws and four guidance pins for the absorber foils was developed, see Fig. 4. Additionally, borosilicate glass slides (0.2 mm×18 mm×18 mm) are used as separating layers to avoid the absorber material from being welded to the press itself. The loaded press is placed in an oven and exposed to a well-defined temperature and pressure—depending on the press design—for a fixed time. For radionuclides material in the form of high melting point carrier salts, such as NaCl, very different diffusion welding process parameters are used—e.g., torque per screw: 2 Nm, oven temperature: 400 °C, process time: 1 h—than for those in the form of low melting point carrier salts, for instance Tc_2O_7, e.g., torque per screw: 10 Nm, oven temperature: 140 °C, process time: 40 h. Excessively high oven temperature could cause melting of the radioactive
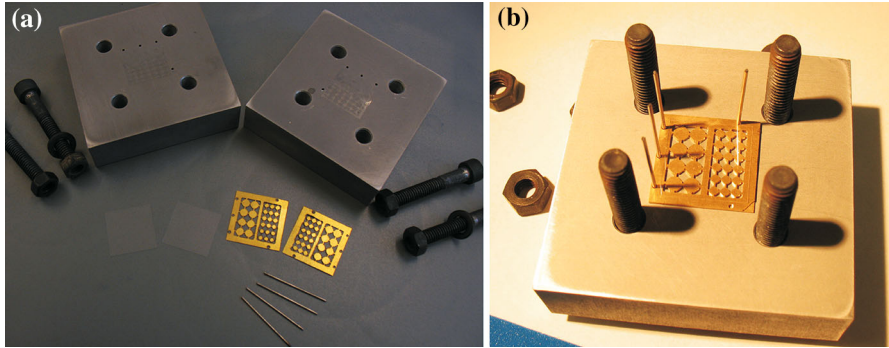
Fig. 4 (Color figure online) **a** The diffusion welding press consisting of two halves of aluminum, four screws and four guidance pins. **b** The lower part of the press with a glass–absorber–source–absorber–glass sandwich and the four guidance pins
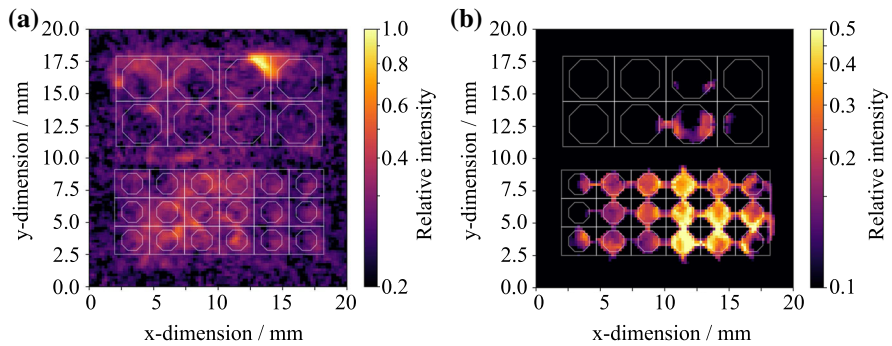

Fig. 5 (Color figure online) Autoradiographic images of two different diffusion welded absorber arrays obtained after 6 days **a** ^{36}Cl absorber array: The emission of bremsstrahlung is seen, but it can also be concluded that the third absorber in the first row is not perfectly sealed and thus cannot be used. **b** ^{99}Tc absorber array: The radioactive material is melted during the diffusion welding and contaminated the absorber surface

material that would lead to leakage of the radioactive material out of the absorber elements.

3 Contamination and Quality Control

Two methods to ensure the complete embedding of the radionuclide material into the absorber after diffusion welding were applied. Firstly, the glass slides are checked for potential radioactive contamination from the above-mentioned leakage using liquid scintillation (LS) counting [12]. The potentially contaminated glass is mixed with a liquid scintillator, and the scintillation photons are counted. Due to the low activities deposited on the absorber array, contaminations, if any, are expected to be small. Therefore, LS sample preparation and the counter should be adapted to low-level measurements. A second means of quality control is autoradiography of the diffusion-

welded source/absorber arrays. Here, the exposure time needs to be significantly larger than for an unsealed source. In Fig. 5, autoradiographic images taken after diffusion welding of (a) ^{36}Cl and (b) ^{99}Tc are shown. From these images, we may conclude which absorbers have been successfully fabricated. In the case of the embedded ^{36}Cl sources, the emission of bremsstrahlung is mainly observed because of the higher electron energies. However, it can also be concluded that the third absorber in the first row is not perfectly sealed and thus cannot be used. For the ^{99}Tc absorber array, see Fig. 5b, a contamination of the gold surface was previously detected via LS counting. Apparently, the radioactive material is melted during the diffusion welding due to the high process temperature of 400 °C resulting in a contamination of the absorber edges which is shown in Fig. 5b.

4 Conclusion

High-quality sources are essential for high-precision radionuclide measurements based on LTDs such as MMC detectors. In this work, we improved source/absorber preparation techniques and established fabrication control methods. The presented techniques have been developed and applied within the EURAMET research project MetroBeta [6–8] for beta emitting radionuclides and will also be employed for electron capture decaying radionuclides within the research project MetroMMC [13].

References

1. A. Fleischmann, Ch. Enss, G.M. Seidel, Top. Appl. Phys. **99**, 151–216 (2005)
2. A. Fleischmann, L. Gastaldo, S. Kempf, A. Kirsch, A. Pabinger, C. Pies, J.-P. Porst, P. Ranitzsch, S. Schäfer, F.V. Seggern, T. Wolf, C. Enss, G.M. Seidel, AIP Conf. Proc. **1185**, 571 (2009). https://doi.org/10.1063/1.3292407
3. S. Kempf, A. Fleischmann, L. Gastaldo, C. Enss, J. Low Temp. Phys. **193**, 365–379 (2018). https://doi.org/10.1007/s10909-014-1190-9
4. H. Rotzinger, M. Linck, A. Burck, M. Rodrigues, M. Loidl, E. Leblanc, L. Fleischmann, A. Fleischmann, C. Enss, J. Low Temp. Phys. **151**, 1087 (2008). https://doi.org/10.1007/s10909-008-9787-5
5. M. Loidl, M. Rodrigues, C. Le-Bret, X. Mougeot, Appl. Radiat. Isot. **87**, 302–305 (2014). https://doi.org/10.1007/s10909-014-1190-9
6. M. Loidl, J. Beyer, L. Bockhorn, C. Enss, D. Györi, S. Kempf, K. Kossert, R. Mariam, O. Nähle, M. Paulsen, M. Rodrigues, M. Schmidt, J. Low Temp. Phys **193**, 1251–1256 (2018). https://doi.org/10.1007/s10909-018-1933-0
7. M. Paulsen, J. Beyer, L. Bockhorn, C. Enss, S. Kempf, K. Kossert, M. Loidl, R. Mariam, O. Nähle, P. Ranitzsch, M. Rodrigues, *JINST*, (accepted), (2019)

8. M. Loidl, J. Beyer, L. Bockhorn, C. Enss, S. Kempf, K. Kossert, R. Mariam, O. Nähle, M. Paulsen, P. Ranitzsch, M. Rodrigues, M. Schmidt, *Appl. Radiat. Isot.*, (submitted), (2019)
9. I. Kawrakow, E. Mainegra-Hing, D.W.O. Rogers, F. Tessier, B.R.B. Walters, *National Research Council Canada*. Technical Report PIRS-701, (2018)
10. F. Schneider, K. Chrysalidis, H. Dorrer, ChE Düllmann, K. Eberhardt, R. Haas, T. Kieck, C. Mokry, P. Naubereit, S. Schmidt, K. Wendt, Nucl. Instrum. Methods Phys. B **376**, 388–392 (2016). https://doi.org/10.1016/j.nimb.2015.12.012
11. N. Barthe, S. Maîtrejean, A. Cardona, Handb. Radioact. Anal. **3**, 1209–1242 (2012). https://doi.org/10.1016/B978-0-12-384873-4.00019-0
12. R. Broda, P. Cassette, K. Kossert, Metrologia **44**, 36–52 (2007). https://doi.org/10.1088/0026-1394/44/4/S06
13. P. C.-O. Ranitzsch, D. Arnold, J. Beyer, L. Bockhorn, J. J. Bonaparte, C. Enss, K. Kossert, S. Kempf, M. Loidl, R. Mariam, O. J. Nähle, M. Paulsen, M. Rodrigues, M. Wegner, *J. Low Temp. Phys.*, This Special Issue, (2019)